Advances in Materials Research, *Vol. 10, No. 2 (2021) 149-168*
DOI: https://doi.org/10.12989/amr.2021.10.2.149

Continuously inhomogeneous beam with longitudinal vertical cracks: an analytical investigation

Victor I. Rizov*

Department of Technical Mechanics, University of Architecture, Civil Engineering and Geodesy, 1 Chr. Smirnensky blvd., 1046 – Sofia, Bulgaria

(*Received August 3, 2020, Revised December 8, 2020, Accepted March 27, 2021*)

Abstract. The present paper is concerned with fracture analysis of an inhomogeneous beam with three longitudinal vertical parallel cracks. The three cracks are located symmetrically with respect to the mid-span. A notch is cut-out in the lateral surface of the beam in the mid-span. Only half of the beam is considered due to the symmetry. The material is continuously inhomogeneous in the width direction of the beam. Besides, the material exhibits non-linear elastic mechanical behavior. The three cracks are located arbitrary in the width direction so as the cross-sections of the four crack arms have different width. The longitudinal fracture behavior is studied in terms of the strain energy release rate. Three solutions to the strain energy release rate are derived by differentiating the complementary strain energy with respect to the areas of the three cracks. The strain energy release rate is determined also by analyzing the balance of the energy for verification. Further verifications are carried-out by applying the *J*-integral approach. The influences of the locations of the three cracks, the material inhomogeneity and the beam geometry on the longitudinal fracture behavior are appraised. Results of analyses of a beam that is continuously inhomogeneous in both width and length directions are also presented.

Keywords: longitudinal vertical crack; continuously inhomogeneous material; non-linear elastic beam; bending; analytical investigation

1. Introduction

Continuously inhomogeneous structural materials are of great interest in development of load-bearing components in various branches of up-to-day engineering. Typically, the properties of inhomogeneous materials vary continuously (smoothly) along one or more directions in the solid (Tokovyy and Ma 2008, 2013, 2017, 2019, Tokovyy 2019). It should be noted that the increased interest towards the inhomogeneous materials in recent decades is due also to the widespread use of certain kinds of inhomogeneous materials such as functionally graded materials (Butcher *et al.* 1999, Dolgov 2002, Gasik 2010, Hedia *et al.* 2014, Mahamood and Akinlabi 2017, Markworth *et al.* 1995, Miyamoto *et al.* 1999, Nemat-Allal *et al.* 2011, Şimşek 2012, 2015, Şimşek *et al.* 2013, Wu *et al.* 2014). Since the functionally graded materials permit controlled tailoring of microstructure and composition during manufacturing, their properties can be formed technologically so as to satisfy various requirements for material properties in different parts of a

*Corresponding author, Professor, E-mail: V_RIZOV_FHE@UACG.BG

http://www.techno-press.org/?journal=amr&subpage=5 ISSN: 2234-0912 (Print), 2234-179X (Online)

structural component.

An important concern for users of inhomogeneous materials is the effect of longitudinal fracture since some inhomogeneous materials such as functionally graded ones can be built-up layer by layer (Mahamood and Akinlabi 2017) which is a premise for appearance of longitudinal cracks between layers. Since longitudinal fracture, i.e., separation of layers, can lead quickly to failure, this phenomenon continues to attract the attention of the scientists and researchers around the globe (Al-Khanbashi and Hamdy 2004, Dolgov 2005, 2016, Her and Su 2015, Klingbeil and Beuth 1997, Tilbrook *et al.* 2005, Yokozeki *et al.* 2008).

Linear-elastic fracture mechanics has been applied to analyze longitudinal fracture (delamination) behavior of various beam structures (Klingbeil and Beuth 1997). The fracture has been studied in terms of the strain energy release rate. Solutions to the strain energy release rate have been obtained assuming linear-elastic behavior of the layered material. The solutions to the strain energy release rate have been used to investigate fracture of several beam configurations of deposited metal layers.

Analyses of delamination fracture of beam configurations have been developed in Yokozeki *et al.* (2008). The methods of linear-elastic fracture mechanics have been used. Solutions to the strain energy release rate have been derived. Results of analyzing the strain energy release rate for different beam geometries and material properties have been reported. It has been found that the solutions can be used in investigations of delamination fracture behavior of layered linear-elastic beams.

Delamination fracture behavior of layered beams has been studied in Her and Su (2015). The strain energy release rate has been analyzed by applying linear-elastic fracture mechanics. The influence of various geometrical parameters and material properties on the fracture behavior of the layered beams has been assessed and discussed in detail.

A study of delamination fracture of a double cantilever beam configuration has been carried-out in Al-Khanbashi and Hamdy (2004). Linear-elastic behavior of the material has been assumed. Delamination under constant load and elevated temperature has been analyzed. The Paris law has been applied for predicting the service lifetime of the structure.

Works on fracture behavior of graded materials have been reviewed in Tilbrook *et al.* (2005). Analyses of fracture under static and fatigue crack loading conditions have been discussed. Studies of cracks oriented both parallel and perpendicular to the direction of material gradient have been summarized. Various fracture analyses by using linear-elastic fracture mechanics have been presented and discussed.

Recently, papers which deal with longitudinal fracture analyses of inhomogeneous beams assuming non-linear mechanical behavior of the material have also been published (Rizov 2016, 2017, 2018, 2019, 2020, Rizov and Altenbach 2020). These papers are focused on beams with one longitudinal crack (Rizov 2016, 2017, 2020). However, the layered structure of inhomogeneous beams favors appearance of more then one parallel longitudinal cracks. Therefore, the objective of the present paper is to develop a fracture analysis of an inhomogeneous non-linear elastic beam with three parallel longitudinal vertical cracks loaded in bending. The fracture is studied in terms of the strain energy release rate by considering the complementary strain energy. The balance of the energy is analyzed for verification. Further verifications of the solutions to the strain energy release rate are performed by applying the J-integral approach.

2. Analytical investigation of the strain energy release rate

An inhomogeneous beam configuration with three longitudinal vertical cracks is shown schematically in Fig. 1. The span of the beam is $2l$. The cross-section of the beam is a rectangle of width, b, and height, h. The beam exhibits continuous material inhomogeneity in the width direction. Besides, the material has non-linear elastic behavior. The loading consists of bending moments, M, applied at the ends of the beam. The lengths of cracks 1, 2 and 3 are $2a_1$, $2a_2$ and $2a_3$, respectively. The length of the front of each crack is h. The three cracks are located symmetrically with respect to the mid-span. Due to the symmetry, only half of the beam, $l \leq x_1 \leq 2l$, is analyzed. In portion, B_1B_2, the three longitudinal cracks divide the beam in four crack arms. The cross-sections of crack arms 1, 2, 3 and 4 are rectangles of widths, b_1, b_2, b_3 and b_4, respectively. A notch of depth, $b_2 + b_3 + b_4$, is cut-out in the mid-span as shown in Fig. 1. The notch divides each of crack arms 2, 3 and 4 in two parts which are symmetric with respect to the mid-span. It is obvious that crack arms 2, 3 and 4 are free of stresses.

The longitudinal fracture behavior is studied in terms of the strain energy release rate, G. First, an elementary increase, da_1, of the length of crack 1 is assumed. The strain energy release rate is written as Rizov (2017)

$$G = 2\frac{dU^*}{hda_1} \tag{1}$$

where the complementary strain energy, U^*, is expressed as

$$U^* = U_1^* + U_{B_2B_3}^* + U_{B_3B_4}^* + U_{UN}^* \tag{2}$$

It should be mentioned that the right-hand side of (1) is doubled in view of the symmetry (Fig. 1). In formula (2), U_1^*, $U_{B_2B_3}^*$, $U_{B_3B_4}^*$ and U_{UN}^* are the complementary strain energies cumulated in crack arm 1, in parts, B_2B_3 and B_3B_4, of the beam and in the un-cracked beam portion, respectively. It should be specified that the boundaries of beam part, B_2B_3, are $x_1 = l + a_1$, $x_1 = l + a_2$, $y_1 = -b/2$ and $y_1 = -b/2 + b_1 + b_2$. The part, B_3B_4, of the beam has the following boundaries: $x_1 = l + a_2$, $x_1 = l + a_3$, $y_1 = -b/2$ and $y_1 = -b/2 + b_1 + b_2 + b_3$. It should also be noted that the complementary strain energy in crack arms 2, 3 and 4 is zero since these crack arms are free of stresses.

The complementary strain energy cumulated in crack arm 1 is written as

$$U_1^* = a_1 \iint_{(A_1)} u_{01}^* dA \tag{3}$$

where u_{01}^* is the complementary strain energy density, A_1 is the area of the cross-section of crack arm 1. In principle, the complementary strain energy density is equal to the area that supplements the area enclosed by the stress-strain curve to a rectangle. Thus, u_{01}^* is expressed as

$$u_{01}^* = \sigma\varepsilon - u_{01} \tag{4}$$

where u_{01} is the strain energy density, σ is the normal stress, ε is the strain.

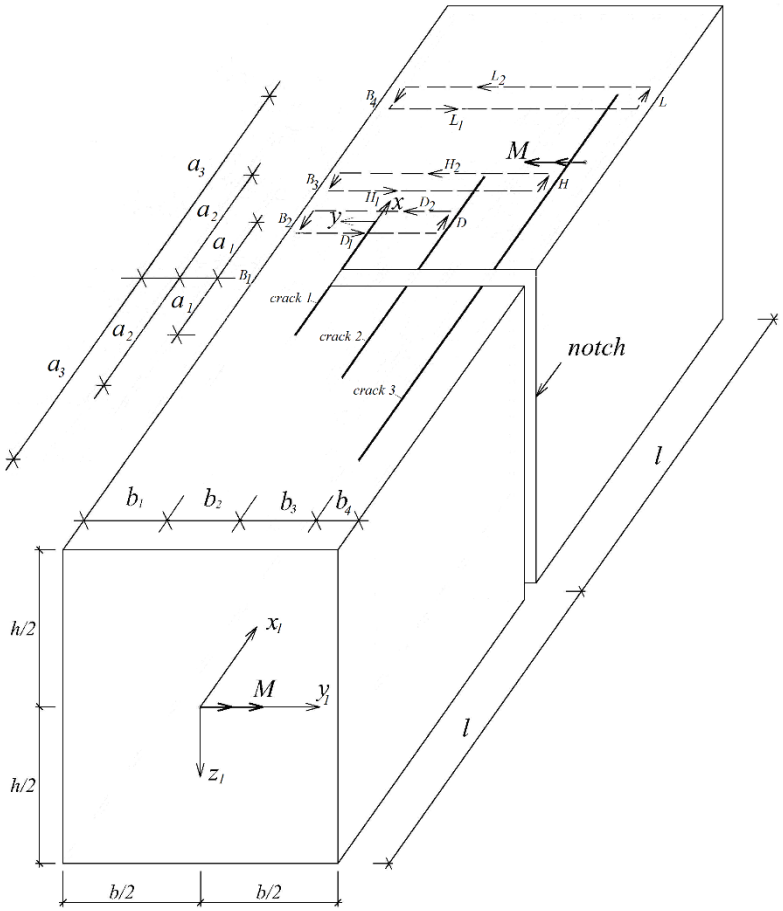

Fig. 1 Geometry and loading of an inhomogeneous beam with three longitudinal vertical cracks

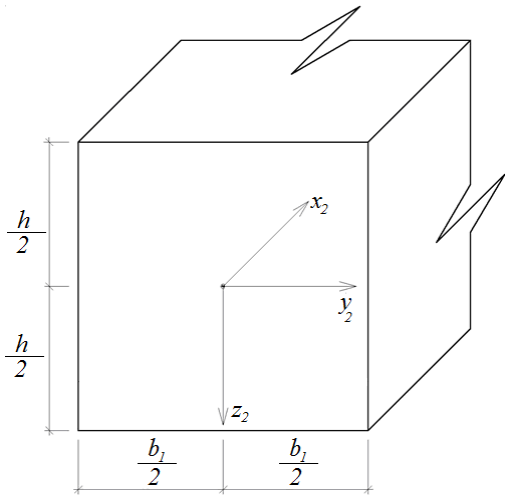

Fig. 2 Cross-section of crack arm 1

The mechanical behavior of the material is treated by applying the following non-linear stress-strain relation (Rudih *et al.* 1998)

$$\sigma = \frac{E\varepsilon}{\sqrt{1+\varepsilon^2}} \tag{5}$$

where E is a material property. The distribution of E along the width of the beam is written as

$$E = E_L e^{f\frac{\frac{b}{2}+y_1}{b}} \tag{6}$$

where

$$-\frac{b}{2} \le y_1 \le \frac{b}{2} \tag{7}$$

In formula (6), E_L is the value of E at the left-hand lateral surface of the beam, f is a material property that controls the material inhomogeneity in the width direction, y_1 is the horizontal centroidal axis (Fig. 1). The strain energy density is derived by integrating of formula (6). The result is

$$u_{01} = E\left(\sqrt{1+\varepsilon^2} - 1\right) \tag{8}$$

By combining of formulae (4), (5) and (8), one obtains

$$u_{01}^{*} = E\left(1 - \frac{1}{\sqrt{1+\varepsilon^2}}\right) \tag{9}$$

Beams of high span to height ratio are under consideration in the present paper. Hence, the distribution of strains is treated by applying Bernoulli's hypothesis for plane sections. Thus, the distribution of strains in the cross-section of crack arm 1 is written as

$$\varepsilon = \kappa_1 z_2 \tag{10}$$

where

$$-\frac{h}{2} \le z_2 \le \frac{h}{2} \tag{11}$$

In formula (10), κ_1 is the curvature of crack arm 1, z_2 is the vertical centroidal axis of the cross-section of crack arm 1 (Fig. 2). The curvature is obtained by using the following equation for equilibrium of elementary forces in the cross-section of crack arm 1

$$\iint_{(A_1)} \sigma z_2 dA = M \tag{12}$$

By using formula (6), the distribution of material property, E, along the width of crack arm 1 is expressed as

$$E = E_L e^{f\frac{\frac{b_1}{2}+y_2}{b}} \tag{13}$$

where y_2 is the horizontal centroidal axis of the cross-section of crack arm 1 (Fig. 2). After substituting of formulae (5), (10) and (13) in Eq. (12), the equation for equilibrium is solved with respect to κ_1 by using the MatLab computer program.

The complementary strain energy cumulated in part, B_2B_3, of the beam are written as

$$U^*_{B_2B_3} = (a_2 - a_1)\iint_{(A_{B_2B_3})} u^*_{0B_2B_3} dA \tag{14}$$

where $u^*_{0B_2B_3}$ is the complementary strain energy density, $A_{B_2B_3}$ is the area of the cross-section of this part of the beam (the width and height of the cross-section are $b_1 + b_2$ and h, respectively). The complementary strain energy density, $u^*_{0B_2B_3}$, is calculated by applying formula (9). For this purpose, ε is replaced with $\varepsilon_{B_2B_3}$ where the distribution of the strains, $\varepsilon_{B_2B_3}$, is found by replacing of κ_1 and z_2 with κ_2 and z_3 in formula (10).

Here κ_2 is the curvature, z_3 is the vertical centroidal axis of the cross-section of part, B_2B_3, of the beam. The equation for equilibrium (12) is used to determine κ_2. For this purpose, b_1 is replaced with $b_1 + b_2$ in formula (13). After substituting of formulae (10) and (13) in Eq. (12), the equation is solved with respect to κ_2 by using the MatLab computer program.

The complementary strain energy density, $u^*_{0B_3B_4}$, is integrated in the volume of part, B_3B_4, of the beam in order to obtain the complementary strain energy

$$U^*_{B_3B_4} = (a_3 - a_2)\iint_{(A_{B_3B_4})} u^*_{0B_3B_4} dA \tag{15}$$

where $A_{B_3B_4}$ is the area of the cross-section of part, B_3B_4 , of the beam (the width and height of the cross-section are $b_1 + b_2 + b_3$ and h, respectively). Formula (9) is applied to determine $u^*_{0B_3B_4}$ by replacing of ε with $\varepsilon_{B_3B_4}$. The distribution of $\varepsilon_{B_3B_4}$ is obtained by replacing of κ_1 and z_2 with κ_3 and z_4, respectively, in formula (10). The curvature, κ_3, of beam part, B_3B_4, is found from the Eq. (12). For this purpose, after replacing of b_1 with $b_1 + b_2 + b_3$ in formula (13) and substituting of formulae (10) and (13) in Eq. (12), the equation for equilibrium is solved with respect to κ_3 by using the MatLab computer program.

The complementary strain energy cumulated in the un-cracked portion of the beam is found by integrating the complementary strain energy density, u^*_{0UN}

$$U^*_{UN} = (l - a_3)\iint_{(A_{UN})} u^*_{0UN} dA \tag{16}$$

where A_{UN} is the area of the cross-section of the beam. The complementary strain energy density, u^*_{0UN}, is obtained by formula (9). For this purpose, ε is replaced with ε_{UN}. Formula (10) is applied to express the distribution of ε_{UN} by replacing of κ_1 and z_2 with κ_4 and z_5, respectively. Here κ_4 and z_5 are the curvature and the vertical centroidal axis in the un-cracked portion of the bream. The equation for equilibrium (12) is used to determine the curvature. For this purpose, b_1 is replaced with b in formula (13). After substituting of formulae (10) and (13) in Eq. (12), the equation is solved with respect to κ_4 by the MatLab computer program.

The following expression for the strain energy release rate is obtained by substituting of

formulae (2), (3), (14), (15) and (16) in formula (1)

$$G = \frac{2}{h}\left(\iint_{(A_1)} u_{01}^{*} dA - \iint_{(A_{B_2B_3})} u_{0B_2B_3}^{*} dA\right) \tag{17}$$

After substituting of the complementary strain energy densities in formula (17), one derives

$$\begin{aligned} G = {} & \frac{2bE_L}{hf}\left(e^{\frac{fb_1}{b}} - 1\right)\left(h + \frac{1}{\kappa_1} ln \frac{-\kappa_1 \frac{h}{2} + \sqrt{\kappa_1^2 \frac{h^2}{4} + 1}}{\kappa_1 \frac{h}{2} + \sqrt{\kappa_1^2 \frac{h^2}{4} + 1}}\right) \\ & - \frac{2bE_L}{hf}\left(e^{\frac{f(b_1+b_2)}{b}} - 1\right)\left(h + \frac{1}{\kappa_2} ln \frac{-\kappa_2 \frac{h}{2} + \sqrt{\kappa_2^2 \frac{h^2}{4} + 1}}{\kappa_2 \frac{h}{2} + \sqrt{\kappa_2^2 \frac{h^2}{4} + 1}}\right) \end{aligned} \tag{18}$$

The strain energy release rate is derived also assuming an elementary increase, da_2, of the length of crack 2. For this purpose, da_1 is replaced with da_2 in formula (1). After substituting of formulae (2), (3), (14), (15) and (16) in formula (1), one obtains

$$G = \frac{2}{h}\left(\iint_{(A_{B_2B_3})} u_{0B_2B_3}^{*} dA - \iint_{(A_{B_3B_4})} u_{0B_3B_4}^{*} dA\right) \tag{19}$$

By combining of formulae (9) and (19), one derives

$$\begin{aligned} G = {} & \frac{2bE_L}{hf}\left(e^{\frac{f(b_1+b_2)}{b}} - 1\right)\left(h + \frac{1}{\kappa_2} ln \frac{-\kappa_2 \frac{h}{2} + \sqrt{\kappa_2^2 \frac{h^2}{4} + 1}}{\kappa_2 \frac{h}{2} + \sqrt{\kappa_2^2 \frac{h^2}{4} + 1}}\right) \\ & - \frac{2bE_L}{hf}\left(e^{\frac{f(b_1+b_2+b_3)}{b}} - 1\right)\left(h + \frac{1}{\kappa_3} ln \frac{-\kappa_3 \frac{h}{2} + \sqrt{\kappa_3^2 \frac{h^2}{4} + 1}}{\kappa_3 \frac{h}{2} + \sqrt{\kappa_3^2 \frac{h^2}{4} + 1}}\right) \end{aligned} \tag{20}$$

Finally, the strain energy release rate is obtained assuming an elementary increase, da_3, of the length of crack 3. By replacing of da_1 with da_3 in formula (1) and substituting of formulae (2), (3), (14), (15) and (16) in formula (1), one derives the following expression for the strain energy release rate

$$G = \frac{2}{h}\left(\iint_{(A_{B_3B_4})} u_{0B_3B_4}^{*} dA - \iint_{(A_{UN})} u_{0UN}^{*} dA\right) \tag{21}$$

After substituting of the complementary strain energy densities in formula (21), the strain energy release rate is obtained as

$$G=\frac{2bE_L}{hf}\left(e^{\frac{f(b_1+b_2+b_3)}{b}}-1\right)\left(h+\frac{1}{\kappa_3}ln\frac{-\kappa_3\frac{h}{2}+\sqrt{\kappa_3^2\frac{h^2}{4}+1}}{\kappa_3\frac{h}{2}+\sqrt{\kappa_3^2\frac{h^2}{4}+1}}\right)$$
$$-\frac{2bE_L}{hf}\left(e^{f}-1\right)\left(h+\frac{1}{\kappa_4}ln\frac{-\kappa_4\frac{h}{2}+\sqrt{\kappa_4^2\frac{h^2}{4}+1}}{\kappa_4\frac{h}{2}+\sqrt{\kappa_4^2\frac{h^2}{4}+1}}\right) \tag{22}$$

For verification, solutions to the strain energy release rate are obtained also by analyzing the balance of the energy. First, crack 1 is considered. A small increase, δa_1, of the length of crack 1 is assumed. The balance of the energy is written as

$$M\delta\phi=\frac{\partial U}{\partial a_1}\delta a_1+Gh\delta a_1 \tag{23}$$

where ϕ is the angle of rotation on the end of the beam (Fig. 3), U is the strain energy. From formula (20), the strain energy release rate is obtained as

$$G=\frac{2}{h}\left(M\frac{\partial\phi}{\partial a_1}-\frac{\partial U}{\partial a_1}\right) \tag{24}$$

It should be mentioned that the expression in brackets in the right-hand side of formula (24) is doubled in view of the symmetry (Fig. 1).

The integrals of Maxwell-Mohr are applied in order to determine the angle of rotation on the end of the beam (Popov 1998). The result is

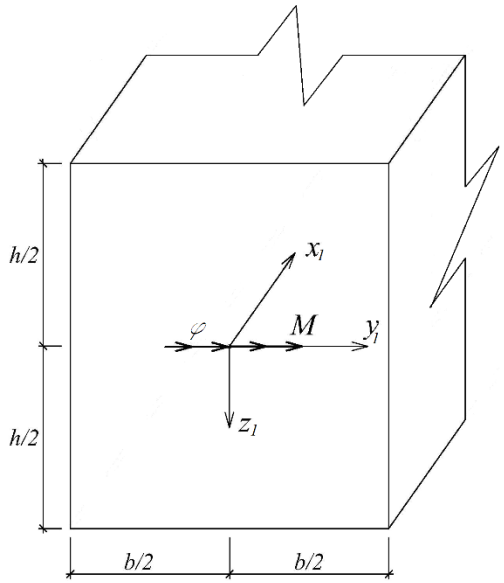

Fig. 3 End section of the beam with angle of rotation and bending moment

$$\phi = \kappa_1 a_1 + \kappa_2(a_2 - a_1) + \kappa_3(a_3 - a_2) + \kappa_4(l - a_3) \tag{25}$$

The strain energy is written as

$$U = U_1 + U_{B_2B_3} + U_{B_3B_4} + U_{UN} \tag{26}$$

U_1, $U_{B_2B_3}$, $U_{B_3B_4}$ and U_{UN} are the strain energies in crack arm 1, in parts, B_2B_3 and B_3B_4, of the beam and in the un-cracked beam portion, respectively. The strain energies, U_1, $U_{B_2B_3}$, $U_{B_3B_4}$ and U_{UN}, are calculated by applying formulae (3), (14), (15) and (16), respectively. For this purpose, the complementary strain energy densities, u_{01}^*, $u_{0B_2B_3}^*$, $u_{0B_3B_4}^*$ and u_{0UN}^*, are replaced with the strain energy densities, u_{01}, $u_{0B_2B_3}$, $u_{0B_3B_4}$ and u_{0UN}, respectively. The strain energy density, u_{01}, is found by formula (8). The strain energy densities, $u_{0B_2B_3}$, $u_{0B_3B_4}$ and u_{0UN}, are derived by replacing of ε, respectively, with $\varepsilon_{B_2B_3}$, $\varepsilon_{B_3B_4}$ and ε_{UN} in formula (8).

By substituting of ϕ and U in formula (24), one obtains

$$G = \frac{2}{h}\left[M(\kappa_1 - \kappa_2) - \iint_{(A_1)} u_{01}dA + \iint_{(A_{B_2B_3})} u_{0B_2B_3}dA\right] \tag{27}$$

Since bending moment can be expressed as a function of stress by the relationship $M = \iint \sigma z\, dA$, formula (27) takes the form

$$G = \frac{2}{h}\left[\iint_{(A_1)} \sigma z_2 \kappa_1 dA - \iint_{(A_{B_2B_3})} \sigma_{B_2B_3} z_3 \kappa_2 dA - \iint_{(A_1)} u_{01}dA + \iint_{(A_{B_2B_3})} u_{0B_2B_3}dA\right] \tag{28}$$

where $\sigma_{B_2B_3}$ is obtained by replacing of ε with $\varepsilon_{B_2B_3}$ in formula (5). The analytical solution of the strain energy release rate derived after substituting of stresses and strain energy densities in formula (28) is exact match of formula (18) which proves the correctness of formula (18).

The strain energy release rate is determined also assuming a small increase, δa_2, of the length of crack 2. For this purpose, by replacing of a_1 with a_2 and substituting of ϕ and U in formula (24), one arrives at

$$G = \frac{2}{h}\left[M(\kappa_2 - \kappa_3) - \iint_{(A_{B_2B_3})} u_{0B_2B_3}dA + \iint_{(A_{B_3B_4})} u_{0B_3B_4}\, dA\right] \tag{29}$$

Formula (29) is re-written as

$$\begin{aligned} G = \frac{2}{h}\Bigg[&\iint_{(A_{B_2B_3})} \sigma_{0B_2B_3} z_3 \kappa_2 dA - \iint_{(A_{B_3B_4})} \sigma_{0B_3B_4} z_4 \kappa_3 dA \\ &- \iint_{(A_{B_2B_3})} u_{0B_2B_3}dA + \iint_{(A_{B_3B_4})} u_{0B_3B_4}\, dA\Bigg] \end{aligned} \tag{3}$$

It should be noted that the analytical solution of (30) matches exactly formula (20). This fact

verifies formula (20).

The strain energy release rate at increase of crack 3 is obtained by replacing of a_1 with a_3 and substituting of ϕ and U in formula (21). The result is

$$G = \frac{2}{h}\left[M(\kappa_3 - \kappa_4) - \iint_{(A_{B_3B_4})} u_{0B_3B_4} dA + \iint_{(A_{UN})} u_{0UN}\, u_{0B_3B_4} dA\right] \tag{31}$$

By using relationship between bending moment and stress, formula (31) is transformed as

$$\begin{aligned} G = \frac{2}{h}\Bigg[&\iint_{(A_{B_3B_4})} \sigma_{B_3B_4} z_4 \kappa_3\, dA - \iint_{(A_{UN})} \sigma_{UN} z_5 \kappa_4\, dA \\ &- \iint_{(A_{B_3B_4})} u_{0B_3B_4}\, dA + \iint_{(A_{UN})} u_{0UN}\, dA\Bigg] \end{aligned} \tag{32}$$

The analytical solution of the strain energy release rate obtained by integrating of (32) is exact match of formula (22) which is a verification of (22).

The longitudinal fracture behavior of the inhomogeneous beam is analyzed also by applying the *J*-integral approach (Broek 1986). First, crack 1 is considered. The integration is performed along the integration contour, *D*, shown by a dashed line in Fig. 1. Since crack arm 2 is free of stresses, the solution to the *J*-integral is written as

$$J = 2\left(J_{D_1} + J_{D_2}\right) \tag{33}$$

where J_{D_1} and J_{D_2} are the values of the *J*-integral is segments, D_1 and D_2, of the integration contour, respectively. Segments, D_1 and D_2, coincide with the cross-sections of crack arm 1 and part, B_2B_3, of the beam, respectively (Fig. 1). It should be noted that the right-hand side of formula (33) is doubled in view of the symmetry.

The *J*-integral in segment, D_1, of the integration contour is written as

$$J_{D_1} = \int_{D_1} \left[u_{01} \cos\alpha - \left(p_x \frac{\partial u}{\partial x} + p_y \frac{\partial v}{\partial x}\right)\right] ds \tag{34}$$

where α is the angle between the outwards normal vector to the contour of integration and the crack direction, p_x and p_y are the components of the stress vector, *u* and *v* are the components of the displacement vector with respect to the coordinate system, *xy*, and ds is a differential element along the contour of integration.

The quantities which are involved in formula (34) are obtained as

$$p_x = -\sigma \tag{35}$$

$$p_y = 0 \tag{36}$$

$$ds = dy_2 \tag{37}$$

$$\cos\alpha = -1 \tag{38}$$

$$\frac{\partial u}{\partial x} = \varepsilon \tag{39}$$

where σ is found by formula (5), the coordinate, y_2, varies in the interval $[-b_1/2; b_1/2]$, the strain, ε, is obtained by formula (10).

In segment, D_2, of the contour of integration, the *J*-integral is written as

$$J_{D_2} = \int_{D_2} \left[u_{0B_2B_3} \cos\alpha_{D_2} - \& \left(p_{x_{D_2}} \frac{\partial u}{\partial x_{D_2}} + p_{y_{D_2}} \frac{\partial v}{\partial x_{D_2}} \right) \right] ds_{D_2} \tag{40}$$

where

$$p_{x_{D_2}} = \sigma_{B_2B_3} \tag{41}$$

$$p_{y_{D_2}} = 0 \tag{42}$$

$$ds_{D_2} = -dy_3 \tag{43}$$

$$\cos\alpha_{D_2} = 1 \tag{44}$$

$$\frac{\partial u}{\partial x_{D_2}} = \varepsilon_{B_2B_3} \tag{45}$$

The stress, $\sigma_{B_2B_3}$, is found by replacing of ε with $\varepsilon_{B_2B_3}$ in the stress-strain relation (5). The coordinate, y_3, varies in the interval $[-(b_1 + b_2)/2; (b_1 + b_2)/2]$.

By substituting of formulae (34) and (40) in formula (33), one arrives at

$$\begin{aligned} J = 2 \int_{D_1} & \left[u_{01} \cos\alpha - \left(p_x \frac{\partial u}{\partial x} + p_y \frac{\partial v}{\partial x} \right) \right] ds \\ & + 2 \int_{D_2} \left[u_{0B_2B_3} \cos\alpha_{D_2} - \left(p_{x_{D_2}} \frac{\partial u}{\partial x_{D_2}} + p_{y_{D_2}} \frac{\partial v}{\partial x_{D_2}} \right) \right] ds_{D_2}. \end{aligned} \tag{46}$$

The average value of the *J*-integral along the front of crack 1 is written as

$$J_{AV} = \frac{1}{h} \int_{-\frac{h}{2}}^{\frac{h}{2}} J dz_2 \tag{47}$$

By combining of formulae (46) and (47), one obtains

$$\begin{aligned} J_{AV} = \frac{2}{h} \Bigg\{ & \int_{-\frac{h}{2}}^{\frac{h}{2}} \int_{D_1} \left[u_{01} \cos\alpha - \left(p_x \frac{\partial u}{\partial x} + p_y \frac{\partial v}{\partial x} \right) \right] ds dz_2 \\ & + \int_{-\frac{h}{2}}^{\frac{h}{2}} \int_{D_2} \left[u_{0B_2B_3} \cos\alpha_{D_2} - \left(p_{x_{D_2}} \frac{\partial u}{\partial x_{D_2}} + p_{y_{D_2}} \frac{\partial v}{\partial x_{D_2}} \right) \right] ds_{D_2} dz_2 \Bigg\} \end{aligned} \tag{48}$$

After substituting of formulae (35)-(39) and (41)-(45) in formula (48), one derives

$$J_{AV}=\frac{2bE_L}{hf}\left(e^{\frac{fb_1}{b}}-1\right)\left(h+\frac{1}{\kappa_1}ln\frac{-\kappa_1\frac{h}{2}+\sqrt{\kappa_1^2\frac{h^2}{4}+1}}{\kappa_1\frac{h}{2}+\sqrt{\kappa_1^2\frac{h^2}{4}+1}}\right)$$
$$-\frac{2bE_L}{hf}\left(e^{\frac{f(b_1+b_2)}{b}}-1\right)\left(h+\frac{1}{\kappa_2}ln\frac{-\kappa_2\frac{h}{2}+\sqrt{\kappa_2^2\frac{h^2}{4}+1}}{\kappa_2\frac{h}{2}+\sqrt{\kappa_2^2\frac{h^2}{4}+1}}\right) \tag{49}$$

The fact that the *J*-integral solution (48) matches exactly the strain energy release rate (18) verifies the analysis of crack 1.

Crack 2 is also analyzed by applying the *J*-integral approach. The integration is carried-out along the integration contour, H, shown by dashed line in Fig. 1. Segments, H_1 and H_2, of the integration contour coincide with the cross-sections of parts, B_2B_3 and B_3B_4, of the beam, respectively. The solution to the *J*-integral along the contour, H, is obtained as

$$J=2\left(J_{H_1}+J_{H_2}\right) \tag{50}$$

where J_{H_1} and J_{H_2} are the *J*-integral values in segments, H_1 and H_2, of the integration contour, respectively. The average value of the *J*-integral along the front of crack 2 is found by using formula (47). For this purpose, formula (50) is re-written as

$$J_{AV}=\frac{2}{h}\left\{\int_{-\frac{h}{2}}^{\frac{h}{2}}\int_{H_1}\left[u_{0B_2B_3}\cos\alpha_{H_1}-\left(p_{x_{H_1}}\frac{\partial u}{\partial x_{H_1}}+p_{y_{H_1}}\frac{\partial v}{\partial x_{H_1}}\right)\right]ds_{H_1}dz_2\right.$$
$$\left.+\int_{-\frac{h}{2}}^{\frac{h}{2}}\int_{H_2}\left[u_{0B_3B_4}\cos\alpha_{H_2}-\left(p_{x_{H_2}}\frac{\partial u}{\partial x_{H_2}}+p_{y_{H_2}}\frac{\partial v}{\partial x_{H_2}}\right)\right]ds_{H_2}dz_2\right\} \tag{51}$$

The quantities involved in formula (51) are obtained as

$$p_{x_{H_1}}=-\sigma_{B_2B_3} \tag{52}$$

$$p_{y_{H_1}}=0 \tag{53}$$

$$ds=dy_3 \tag{54}$$

$$\cos\alpha_{H_1}=-1 \tag{55}$$

$$\frac{\partial u}{\partial x_{H_1}}=\varepsilon_{B_2B_3} \tag{56}$$

$$p_{x_{H_2}}=\sigma_{B_3B_4} \tag{57}$$

$$p_{y_{H_2}} = 0 \tag{58}$$

$$ds_{H_2} = -dy_4 \tag{59}$$

$$cos\,\alpha_{H_2} = 1 \tag{60}$$

$$\frac{\partial u}{\partial x_{H_2}} = \varepsilon_{B_3B_4} \tag{61}$$

where $\sigma_{B_3B_4}$ is found by replacing of ε with $\varepsilon_{B_3B_4}$ in formula (5), the coordinate, y_4, varies in the interval $[-(b_1+b_2+b_3)/2;(b_1+b_2+b_3)/2]$. After substituting of formulae (52)-(61) in formula (51), the solution of the *J*-integral is found as

$$\begin{aligned} J_{AV} = {} & \frac{2bE_L}{hf}\left(e^{\frac{f(b_1+b_2)}{b}}-1\right)\left(h+\frac{1}{\kappa_2}ln\frac{-\kappa_2\frac{h}{2}+\sqrt{\kappa_2^2\frac{h^2}{4}+1}}{\kappa_2\frac{h}{2}+\sqrt{\kappa_2^2\frac{h^2}{4}+1}}\right) \\ & -\frac{2bE_L}{hf}\left(e^{\frac{f(b_1+b_2+b_3)}{b}}-1\right)\left(h+\frac{1}{\kappa_3}ln\frac{-\kappa_3\frac{h}{2}+\sqrt{\kappa_3^2\frac{h^2}{4}+1}}{\kappa_3\frac{h}{2}+\sqrt{\kappa_3^2\frac{h^2}{4}+1}}\right) \end{aligned} \tag{62}$$

The *J*-integral solution (62) is exact match of the strain energy release rate (20). This is a verification of formula (20).

Finally, the *J*-integral approach is used also to analyze crack 3. The integration is performed along the contour, L, shown by dashed line in Fig. 1. The *J*-integral solution is written as

$$J = 2\left(J_{L_1}+J_{L_2}\right) \tag{63}$$

where J_{L_1} and J_{L_2} are the *J*-integral values in segments, L_1 and L_2, of the integration contour, respectively. Segments, L_1 and L_2, coincide with the cross-sections of beam part, B_3B_4, and the un-cracked portion of the beam, respectively. By using formula (47), the average value of the *J*-integral along the front of crack 3 is expressed as

$$\begin{aligned} J_{AV} = \frac{2}{h}\Bigg\{ & \int_{-\frac{h}{2}}^{\frac{h}{2}}\int_{L_1}\left[u_{0B_3B_4}\,cos\,\alpha_{L_1}-\left(p_{x_{L_1}}\frac{\partial u}{\partial x_{L_1}}+p_{y_{L_1}}\frac{\partial v}{\partial x_{L_1}}\right)\right]ds_{L_1}dz_2 \\ & +\int_{-\frac{h}{2}}^{\frac{h}{2}}\int_{L_2}\left[u_{0UN}\,cos\,\alpha_{L_2}-\&\left(p_{x_{L_2}}\frac{\partial u}{\partial x_{L_2}}+p_{y_{L_2}}\frac{\partial v}{\partial x_{L_2}}\right)\right]ds_{L_2}dz_2\Bigg\} \end{aligned} \tag{64}$$

The quantities involved in formula (64) are written as

$$p_{x_{L_1}} = -\sigma_{B_3B_4} \tag{65}$$

$$p_{y_{L_1}} = 0 \tag{66}$$

$$ds = dy_4 \tag{67}$$

$$cos\,\alpha_{L_1} = -1 \tag{68}$$

$$\frac{\partial u}{\partial x_{L_1}} = \varepsilon_{B_3B_4} \tag{69}$$

$$p_{x_{L_2}} = \sigma_{UN} \tag{70}$$

$$p_{y_{L_2}} = 0 \tag{71}$$

$$ds_{L_2} = -dy_5 \tag{72}$$

$$cos\,\alpha_{L_2} = 1 \tag{73}$$

$$\frac{\partial u}{\partial x_{L_2}} = \varepsilon_{UN} \tag{74}$$

where the stress, σ_{UN}, is found by replacing of ε with ε_{UN} in formula (5), the coordinate, y_5, varies in the interval $[-b/2; b/2]$. By combining of formulae (64)-(74), one obtains

$$\begin{aligned} J_{AV} = {} & \frac{2bE_L}{hf}\left(e^{\frac{f(b_1+b_2+b_3)}{b}} - 1\right)\left(h + \frac{1}{\kappa_3} ln \frac{-\kappa_3 \frac{h}{2} + \sqrt{\kappa_3^2 \frac{h^2}{4} + 1}}{\kappa_3 \frac{h}{2} + \sqrt{\kappa_3^2 \frac{h^2}{4} + 1}}\right) \\ & - \frac{2bE_L}{hf}\left(e^f - 1\right)\left(h + \frac{1}{\kappa_4} ln \frac{-\kappa_4 \frac{h}{2} + \sqrt{\kappa_4^2 \frac{h^2}{4} + 1}}{\kappa_4 \frac{h}{2} + \sqrt{\kappa_4^2 \frac{h^2}{4} + 1}}\right) \end{aligned} \tag{75}$$

The fact that the *J*-integral (75) matches exactly the strain energy release rate (22) confirms the correctness of the analysis of crack 3.

It should be mentioned that from computational view point, benefit of using of formulae (17), (19) and (21) consists in the fact that the strain energy release rate can be calculated simply by integrating of the complementary strain energy density. This method has its advantages over other methods such as the method by analyzing of the balance of the energy and the *J*-integral method. For example, the solution of the strain energy release rate by analyzing of the balance of the energy requires integrations of the both stresses and the strain energy densities. The application of the *J*-integral method requires determination of the components of the integral. The method presented here is particularly beneficial in case of a beam with more parallel longitudinal cracks.

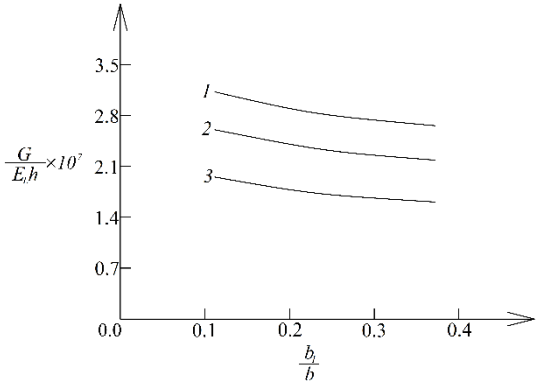

Fig. 4 The strain energy release rate in non-dimensional form plotted against b_1/b ratio (curve 1 – at $h/b = 1.5$, curve 2 – at $h/b = 1.6$ and curve 3 – at $h/b = 1.7$)

3. Numerical example

The present section of the paper contains numerical results obtained by applying the solutions to the strain energy release rate derived in the previous section. The strain energy release rate is presented in non-dimensional form by using the formula $G_N = G/(E_L h)$. The numerical results are used to evaluate the influence of material inhomogeneity, locations of the three cracks in the width direction of the beam and the geometry of the beam on the longitudinal fracture behavior. It is assumed that $b = 0.02$ m, $h = 0.03$ m and $M = 4$ Nm.

The location of crack 1 along the beam width is characterized by b_1/b ratio. In order to assess the influence of location of crack 1 on the longitudinal fracture behavior of the beam, the strain energy release rate obtained at increase of crack 1 is plotted in non-dimensional form against b_1/b ratio in Fig. 4 at three h/b ratios for $(b_1 + b_2)/b = 0.5$ and $(b_1 + b_2 + b_3)/b = 0.8$. The curves in Fig. 4 indicate that the strain energy release rate decreases with increasing of b_1/b ratio. This finding is attributed to the increase of the stiffness of crack arm 1. It can be observed also in Fig. 4 that the strain energy release rate decreases with increasing of h/b ratio (this behavior is due to increase of the stiffness of the beam).

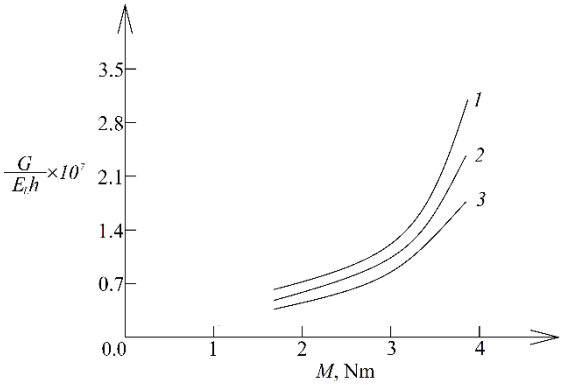

Fig. 5 The strain energy release rate in non-dimensional form plotted against M (curve 1 – at $(b_1 + b_2)/b = 0.5$, curve 2 – at $(b_1 + b_2)/b = 0.6$ and curve 3 – at $(b_1 + b_2)/b = 0.7$)

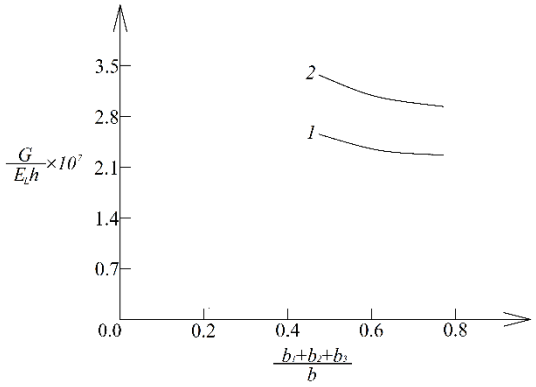

Fig. 6 The strain energy release rate in non-dimensional form plotted against $(b_1 + b_2 + b_3)/b$ ratio (curve 1 – at $M = 3$ Nm and curve 2 – at $M = 4$ Nm)

The ratio, $(b_1 + b_2)/b$, is used to characterize the location of crack 2 along the width of the beam. One can get an idea for the influence of the location of crack 2 along the beam width on the longitudinal behavior from Fig. 5 where the strain energy release rate obtained at increase of crack 2 is plotted in non-dimensional form against the bending moment, M, at three $(b_1 + b_2)/b$ ratios for $b_1/b = 0.2$ and $(b_1 + b_2 + b_3)/b = 0.8$.

One can observe in Fig. 5 that the strain energy release rate decreases with increasing of $(b_1 + b_2)/b$ ratio.

The effect of the location of crack 3 along the width of the beam is appraised too. The location of crack 3 is characterized by $(b_1 + b_2 + b_3)/b$ ratio. The strain energy release rate obtained at increase of crack 3 is plotted in non-dimensional form against $(b_1 + b_2 + b_3)/b$ ratio in Fig. 6 at two values of M for $b_1/b = 0.2$ and $(b_1 + b_2)/b = 0.5$. It can be observed in Fig. 6 that the strain energy release rate decreases with increasing of $(b_1 + b_2 + b_3)/b$ ratio.

The influence of the material inhomogeneity in the width direction of the beam on the longitudinal fracture behavior is also evaluated.

The material inhomogeneity is characterized by material property, f. In order to evaluate the influence of f, the strain energy release rate obtained by using solutions (18), (20) and (22) which

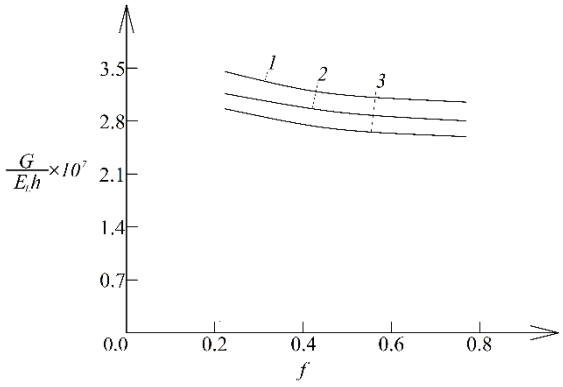

Fig. 7 The strain energy release rate in non-dimensional form plotted against f (curve 1 – at increase of crack 1, curve 2 – at increase of crack 2 and curve 3 – at increase of crack 3)

are derived, respectively, at increase of cracks 1, 2 and 3 is plotted in non-dimensional form against f in Fig. 7. The curves in Fig. 7 show that the strain energy release rate decreases with increasing of f.

One can observe also in Fig. 7 that the strain energy release rate obtained at increase of crack 1 is higher than these obtained at increase of cracks 2 and 3. The strain energy release rate obtained at increase of crack 3 is lower than these found at increase of cracks 2 and 3. The strain energy release rate obtained at increase of crack 2 has intermediate value with respect to these obtained at increase of cracks 1 and 2 (Fig. 7).

It should be mentioned that the solutions to the strain energy release rate and the *J*-integral derived in the present paper can also be applied when the beam exhibit1s continuous material inhomogeneity in both width and length directions. For this purpose, the value of material property, E_L, has to be obtained at the length of the crack under consideration. It is assumed that the material property, E_L, is distributed along the beam length according to the following law

$$E_L = E_{LN} e^{r\frac{x_1}{l}} \tag{76}$$

at

$$0 \leq x_1 \leq l \tag{77}$$

and

$$E_L = E_{LN} e^{r\frac{(2l-x_1)}{l}} \tag{78}$$

at

$$l \leq x_1 \leq 2l \tag{79}$$

In formulae (76) and (78), r is a material property that controls the inhomogeneity in the length direction of the beam, E_{LN} is the value of E_L in the ends of the beam. Formulae (76) and (78) indicate that E_L is distributed symmetrically with respect to the mid-span.

The influence of material property, r, on the longitudinal fracture behavior of the beam is illustrated in Fig. 8 where the strain energy release rate obtained at increase of crack 3 is plotted in

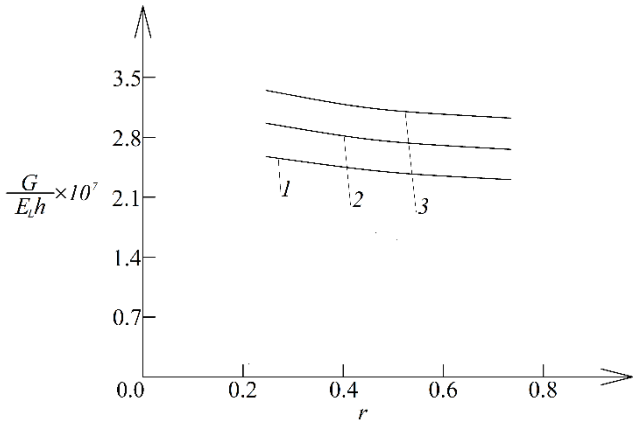

Fig. 8 The strain energy release rate in non-dimensional form plotted against r (curve 1 – at $a_3/l = 0.5$, curve 2 – at $a_3/l = 0.6$ and curve 3 – at $a_3/l = 0.7$)

non-dimensional form against the material property, r, at three a_3/l ratios. The curves in Fig. 8 indicate that the strain energy release rate decreases with increasing of r. It can also be observed in Fig. 8 that the increase of a_3/l ratio leads to increase of the strain energy release rate.

4. Conclusions

The fracture behavior of an inhomogeneous beam with three parallel longitudinal vertical cracks is analyzed. The beam exhibits continuous material inhomogeneity in the width direction. The material has non-linear elastic mechanical behavior. The external loading consists of bending moments applied at the ends of the beam. The three cracks are located symmetrically with respect to the mid-span. Thus, only half of the beam is analyzed. A notch is cut-out in the mid-span so as the crack arms 2, 3 and 4 are free of stresses. The cracks are located arbitrary in the width direction of the beam. Hence, the widths of the cross-sections of the four crack arms are different. The three cracks have different lengths. The longitudinal fracture behavior is studied in terms of the strain energy release rate. Solutions to the strain energy release rate are derived by differentiating the complementary strain energy in the beam with respect to the areas of the cracks. In order to verify these solutions, the strain energy release rate is obtained also by analyzing the balance of the energy. The solutions to the strain energy release rate are verified further by applying the *J*-integral approach. The solutions to the strain energy release rate are used to appraise the influence of material inhomogeneity, the location of the three cracks in the width direction of the beam, the external loading and the beam geometry on the longitudinal fracture behavior. The locations of cracks 1, 2 and 3 in the width direction are characterized by b_1/b, $(b_1+b_2)/b$ and $(b_1+b_2+b_3)/b$ ratios, respectively. The analysis reveals that the strain energy release rate decreases with increasing of b_1/b, $(b_1+b_2)/b$ and $(b_1+b_2+b_3)/b$ ratios. The material inhomogeneity along the width of the beam is characterized by material property, f. It is found that the strain energy release rate decreases with increasing of f. This finding is attributed to the increase of the stiffness of the beam. The increase of h/b ratio also leads to decrease of the strain energy release rate. The calculations indicate that the strain energy release rate derived at increase of crack 1 is higher in comparison to these derived at increase of crack 2 and crack 3. The strain energy release rate at increase of crack 3 is lower than these at increase of crack 1 and crack 2. The strain energy release rate obtained at increase of crack 2 has intermediate value with respect to these obtained at increase of crack 1 and crack 3. The solutions to the strain energy release rate and the *J*-integral derived in the present paper can be applied also when the beam exhibit continuous material inhomogeneity in both width and length directions. The material inhomogeneity in the length direction is characterized by material property, r. The analysis shows that the strain energy release rate decreases with increasing of r. Concerning the influence of the crack length on the longitudinal fracture behavior, it is found that when the beam is inhomogeneous in width and length directions, the strain energy release rate increases with increasing of a_3/l ratio. It should be noted that the approach developed in the present paper may calculate also the adhesion energy of single-layer coatings with a gradient of elastic properties in thickness or of two-layer and three-layer coatings.

References

Al-Khanbashi, A. and Hamdy, A.E. (2004), "Fracture mechanics approach to predict delamination lifetime in Mode II under constant loads", *J. Adhes. Sci. Technol.*, **18**, 227-242. https://doi.org/10.1163/156856104772759430

Broek, D. (1986), *Elementary Engineering Fracture Mechanics*, Springer.

Butcher, R.J., Rousseau, C.E. and Tippur, H.V. (1998), "A functionally graded particulate composite: Measurements and Failure Analysis", *Acta. Mater.*, **47**(1), 259-268. https://doi.org/10.1016/S1359-6454(98)00305-X

Dolgov, N.A. (2002), "Effect of the elastic modulus of a coating on the serviceability of the substrate-coating system", *Strength Mater.*, **34**(2), 153-157. https://doi.org/10.1007/s11223-005-0053-7

Dolgov, N.A. (2005), "Determination of stresses in a two-layer coating", *Strength Mater.*, **37**(2), 422-431. https://doi.org/10.1007/s11223-005-0053-7

Dolgov, N.A. (2016), "Analytical methods to determine the stress state in the substrate–coating system under mechanical loads", *Strength Mater.*, **48**(1), 658-667. https://doi.org/10.1007/s11223-016-9809-5

Gasik, M.M. (2010), "Functionally graded materials: bulk processing techniques", *Int. J. Mater. Product Technol.*, **39**(1-2), 20-29. https://doi.org/10.1504/IJMPT.2010.034257

Hedia, H.S., Aldousari, S.M., Abdellatif, A.K. and Fouda, N.A. (2014), "New design of cemented stem using functionally graded materials (FGM)", *Biomed. Mater. Eng.*, **24**(3), 1575-1588. https://doi.org/10.3233/BME-140962

Her, S.C. and Su, W.B. (2015), "Interfacial fracture toughness of multilayered composite structures", *Strength Mater.*, **47**(1), 186-191. https://doi.org/10.1007/s11223-015-9646-y

Klingbeil, N.W. and Beuth, J.I. (1997), "Interfacial fracture testing of deposited metal layers under four-point bending", *Eng. Fract. Mech.*, **56**, 113-126. https://doi.org/10.1016/S0013-7944(96)00109-9

Mahamood, R.M. and Akinlabi, E.T. (2017), *Functionally Graded Materials*, Springer.

Markworth, A.J., Ramesh, K.S. and Parks, W.P. (1995), "Review: modeling studies applied to functionally graded materials", *J. Mater. Sci.*, **30**(3), 2183-2193. https://doi.org/10.1007/BF01184560

Miyamoto, Y., Kaysser, W.A., Rabin, B.H., Kawasaki, A. and Ford, R.G. (1999), *Functionally Graded Materials: Design, Processing and Applications*, Kluwer Academic Publishers, Dordrecht/London/Boston.

Nemat-Allal, M.M., Ata, M.H., Bayoumi, M.R. and Khair-Eldeen, W. (2011), "Powder metallurgical fabrication and microstructural investigations of Aluminum/Steel functionally graded material", *Mater. Sci. Applicat.*, **2**(5), 1708-1718. https://doi.org/10.4236/msa.2011.212228

Popov, E.P. (1998), *Engineering Mechanics of Solids*, Pearson.

Rizov, V.I. (2016), "Elastic-plastic fracture of functionally graded circular shafts in torsion", *Adv. Mater. Res., Int. J.*, **5**(4), 299-318. https://doi.org/10.12989/amr.2016.5.4.299

Rizov, V.I. (2017), "Analysis of longitudinal cracked two-dimensional functionally graded beams exhibiting material non-linearity", *Frattura ed Integrità Strutturale*, **41**, 498-510. https://doi.org/10.3221/IGF-SIS.41.61

Rizov, V.I. (2018), "Analysis of cylindrical delamination cracks in multilayered functionally graded non-linear elastic circular shafts under combined loads", *Frattura ed Integrità Strutturale*, **46**, 158-177. https://doi.org/10.3221/IGF-ESIS.46.16

Rizov, V.I. (2019), "Influence of material inhomogeneity and non-linear mechanical behavior of the material on delamination in multilayered beams", *Frattura ed Integrità Strutturale*, **47**, 468-481. https://doi.org/10.3221/IGF-ESIS.47.37

Rizov, V.I. (2020), "Longitudinal fracture analysis of inhomogeneous beams with continuously changing radius of cross-section along the beam length", *Strength Fract. Complex.: Int. J.*, **13**, 31-43. https://doi.org/10.3233/SFC-200250

Rizov, V. and Altenbach, H. (2020), "Longitudinal fracture analysis of inhomogeneous beams with continuously varying sizes of the cross-section along the beam length", *Frattura ed Integrità Strutturale*, **53**, 38-50. https://doi.org/10.3221/IGF-ESIS.53.04

Rudih, O.L., Sokolov, G.P. and Pahomov, V.L. (1998), "Introduction to non-linear structural mechanics", IASV, Moscow, Russia.

Şimşek, M. (2012), "Nonlocal effects in the free longitudinal vibration of axially functionally graded tapered nanorods", *Computat. Mater. Sci.*, **61**, 257-265. https://doi.org/10.1016/j.commatsci.2012.04.001

Şimşek, M. (2015), "Bi-directional functionally graded materials (BDFGMs) for free and forced vibration of Timoshenko beams with various boundary conditions", *Compos. Struct.*, **133**, 968-978. https://doi.org/10.1016/j.compstruct.2015.08.021

Şimşek, M., Kocatürk, T. and Akbaş, D. (2013), "Static bending of a functionally graded microscale Timoshenko beam based on the modified couple stress theory", *Compos. Struct.*, **95**, 740-747. https://doi.org/10.1016/j.compstruct.2012.08.036

Tilbrook, M.T., Moon, R.J. and Hoffman, M. (2005), "Crack propagation in graded composites", *Compos. Sci. Technol.*, **65**(2), 201-220. https://doi.org/10.1016/j.compscitech.2004.07.004

Tokovyy, Y. (2019), "Solutions of axisymmetric problems of elasticity and thermoelasticity for an inhomogeneous space and a half space", *J. Mathe. Sci.*, **240**(1), 86-97. https://doi.org/10.1007/s10958-019-04337-3

Tokovyy, Y. and Ma, C.C. (2008), "Analysis of 2D non-axisymmetric elasticity and thermoelasticity problems for radially inhomogeneous hollow cylinders", *J. Eng. Math*., **61**(3), 171-184. https://doi.org/10.1007/s10665-007-9154-6

Tokovyy, Y. and Ma, C.C. (2013), "Three-dimensional temperature and thermal stress analysis of an inhomogeneous layer", *J. Thermal Stress.*, **36**(2), 790-808. https://doi.org/10.1080/01495739.2013.787853

Tokovyy, Y. and Ma, C.C. (2017), "Three-dimensional elastic analysis of transversely-isotropic composites", *J. Mech.*, **33**(6), 821-830. https://doi.org/10.1017/jmech.2017.91

Tokovyy, Y. and Ma, C.C. (2019), "Elastic analysis of inhomogeneous solids: History and development in brief", *J. Mech.*, **18**(1), 1-14. https://doi.org/10.1017/jmech.2018.57

Wu, X.L., Jiang, P., Chen, L., Zhang, J.F., Yuan, F.P. and Zhu, Y.T. (2014), "Synergetic strengthening by gradient structure", *Mater. Res. Lett*., **2**(1), 185-191. https://doi.org/10.1080/21663831.2014.935821

Yokozeki, T, Ogasawara, T. and Aoki, T. (2008), "Correction method for evaluation of interfacial fracture toughness of DCB, ENF and MMB specimens with residual thermal stresses", *Compos. Sci. Technol*., **68**, 760-767. https://doi.org/10.1016/j.compscitech.2007.08.025

CC